Analytica Chimica Acta 1134 (2020) 10–17

Contents lists available at ScienceDirect

Analytica Chimica Acta

journal homepage: www.elsevier.com/locate/aca

Target Induced-DNA strand displacement reaction using gold nanoparticle labeling for hepatitis E virus detection

Tatchanun Ngamdee [a], Lee Su Yin [b], Sompong Vongpunsawad [c], Yong Poovorawan [c], Werasak Surareungchai [a, d], Benchaporn Lertanantawong [d, e, *]

[a] Department of Biotechnology, School of Bioresources and Technology, King Mongkut's University of Technology Thonburi, Bangkok, 10150, Thailand
[b] Faculty of Applied Sciences, AIMST University, Bedong, Kedah, 08100, Malaysia
[c] Center of Excellence in Clinical Virology, Faculty of Medicine, Chulalongkorn University, Bangkok, 10330, Thailand
[d] Nanoscience and Nanotechnology Program, King Mongkut's University of Technology Thonburi (KMUTT), Bangkok, 10140, Thailand
[e] Department of Biomedical Engineering, Faculty of Engineering, Mahidol University, Salaya, Nakhon Pathom, 73170, Thailand

HIGHLIGHTS

- One-pot detection with femtomolar limit of detection.
- Signal interpretation can be achieved in three ways, visual observation, spectrophotometry, and electrochemical detection.
- The integration of lyophilization and magnetogenosensing makes the test stable and easy to transport.
- This platform can potentially detect nucleic acid of any viral or bacterial pathogen in infected samples.

GRAPHICAL ABSTRACT

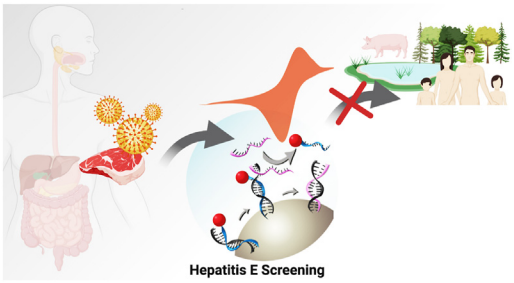

ARTICLE INFO

Article history:
Received 28 May 2020
Received in revised form
8 August 2020
Accepted 11 August 2020
Available online 21 August 2020

Keywords:
DNA strand displacement
One-pot detection
No-wash biosensor
Gold reporter probe
Hepatitis E virus

ABSTRACT

DNA strand displacement is an attractive, enzyme-free target hybridization strategy for nano-biosensing. The target DNA induces a strand displacement reaction by replacing the pre-hybridized strand that is labeled with gold nanoparticles (AuNPs). Thus, the amount of displaced-AuNP-labeled strand is proportional to the amount of target DNA in the sample. The use of a magnetogenosensing technique to isolate the target DNA allows for a simple, one-pot detection approach, which minimizes possible carry-over contamination and pipetting errors. We sought a proof-of-concept for this technology in its ability to detect DNA-equivalent of hepatitis E virus (HEV), which causes acute viral hepatitis for which rapid and simple diagnostic methods remain limited. Signal detection was done via visual observation, spectrophotometry, and electrochemistry. The sensor demonstrated good sensitivity with detection limits of 10 pM (visual), 10 pM (spectrophotometry) and 1 fM (electrochemical). This sensor also exhibited high specificity for real target amplicons and could discriminate between perfect and mismatched sequences. Lyophilized biosensor reagents stored at 4 °C, 25 °C, and outdoor ambient temperature, were stable for up to 90, 50, and 40 days, respectively. The integration of magnetic separation and target DNA-induced strand displacement reaction in a dry reagent form makes the sensing platform easy-to-use and suitable for field settings.

* Corresponding author. Department of Biomedical Engineering, Faculty of Engineering, Mahidol University, Salaya, Nakhon Pathom, Thailand.
E-mail address: benchaporn.ler@mahidol.ac.th (B. Lertanantawong).

https://doi.org/10.1016/j.aca.2020.08.018
0003-2670/

1. Introduction

Infections caused by hepatitis E virus (HEV) is emerging as a serious global disease. It is transmitted via the fecal-oral route, mainly through contaminated food and water. HEV infection is associated with several extrahepatic manifestations, including a range of neurological injuries, pancreatitis, kidney injury, thrombocytopenia and death in severe cases. There is currently no universally approved vaccine for HEV [1,2]. Therefore, timely detection of the disease is important, particularly in under-resourced, endemic, or high-burden areas. Several HEV detection assays have been developed, such as Polymerase chain reaction (PCR) [3–8], Next-generation sequencing (NGS) [9], Enzyme-linked immunosorbent assay (ELISA) [10,11] and Loop-mediated isothermal amplification (LAMP) [12,13]. These methods achieve ultra-sensitivity, but the stability and cost of the enzymes often limit its utility.

Electrochemistry-based DNA biosensors offer many advantages as an alternate HEV screening assay, as they are highly sensitive, simple, portable and cost-effective for nucleic acid detection [14]. Gold nanoparticles (AuNPs) are commonly used as an electrochemical label for nucleic acid assays owing to their favorable characteristics such as facile chemical synthesis with well-controlled nano-scaled particle and size distribution, wide compatibility with biomolecules, and high stability [15,16]. The use of magnetic bead nanoparticles (MBs) or Fe_3O_4 (ferro/ferric oxide) nanoparticles for molecular separation and purification of nucleic acids eliminates the complicated procedures of conventional solid-phase DNA isolation [17,18]. In addition, the MBs provide a large surface area for the attachment of prehybridized DNA strands in the target induced-DNA strand displacement reaction.

Target induced-DNA strand displacement is a DNA hybridization strategy whereby one of the double-stranded target DNA strands displaces a prehybridized strand so that it can bind to the free strand that is partially or fully complementary to it [19–21]. Strand displacement can be initiated at complementary single-stranded domains or toehold and progresses simultaneously through branch migration. A displacement reaction is a spontaneous reaction that does not require external energy or an enzyme. The reaction rate can be accelerated by changing the temperature or salt concentration. This reaction has been integrated into applications such as isothermal DNA amplification [22], nano-machine or DNA walker [23], controllable immobilization of enzymes [20], and DNA sensing [19,24].

This paper describes the one-pot detection of HEV using a DNA strand displacement reaction. As illustrated in Scheme 1, there are 4 main steps in this process. Firstly, AuNP-labeled reporter probes (RP) are pre-hybridized with capture probes (CP) on MBs. In the presence of target DNA, the target strand that is complementary to the CP will displace the AuNP-labeled RP and bind to the CP. The unbound AuNP-labeled RP will be separated from the MB-CP-bound RP using magnetic separation. The number of displaced AuNP-RP represents the amount of target DNA. Signal detection can be done by visual observation, spectrophotometry or electrochemical detection. Furthermore, a hybridization mix containing all reagents, except the DNA target, was lyophilized into a ready-to-use dry form for long term stability and storage.

2. Material and methods

2.1. Reagents and materials

All solutions were prepared with ultrapure water from Milli-Q® Integral Water Purification System (Merck, Germany). Sodium chloride, potassium chloride, sodium phosphate dibasic, potassium dihydrogen phosphate, Tween 20, sorbitol, sucrose, tris-base, acetic acid, sodium dodecyl sulphate (SDS) and tris (2-carboxyethyl) phosphine (TCEP) were purchased from Sigma-Aldrich, USA. Dynabeads™ MyOne™ Streptavidin T1 were purchased from Thermo Fisher Scientific, USA and 40 nm gold nanoparticles were purchased from DCN Diagnostics, USA. Screen-printed carbon electrodes (SPCE) were obtained from Quasense, Thailand.

All oligonucleotides used in this work were supplied by Integrated DNA Technologies, USA. The capture and biotin blocking probes are labeled with biotin at the 5′ ends, while the reporter and thiol blocking probes are labeled with thiol group at the 5’ ends. The details of the sequences are listed in Table 1.

2.2. DNA conjugation to AuNPs

Functionalization of AuNPs with thiolated oligonucleotides was performed using the salt ageing method with a slight modification [25]. Firstly, 10 μL of RP (100 μM) and 30 μL of thiol blocking probes (100 μM) were activated by TCEP. Then, the thiol-activated probes were added to 1 mL of a 40 nm AuNPs solution and allowed to incubate for 16 h at room temperature. After incubation, 10 μL of 500 mM Tris-acetate (pH 8.2) and 100 μL of 1 M NaCl were added into the mixture. The reaction mixture was incubated for at least 24 h at room temperature to complete the conjugation process. After centrifugation, the AuNP-conjugated probes (AuNP-RP) were resuspended with 500 μL of 25 mM Tris-acetate with 8% (w/v) sucrose buffer (pH 7.4) and kept at 4 °C until use.

2.3. DNA immobilization on MB nanoparticles

The immobilization of DNA on the MB was performed according to the manufacturer’s instructions. 100 μL of Dynabead™ MyOne™ Streptavidin T1 (10 μg μL^{-1}) was washed 3 times with 20 mM PBS (pH 7.4) containing 0.05% Tween 20. After that, 4 μL of CP (100 μM) and 12 μL of biotin blocking probe (100 μM) were added to the MBs and incubated for 40 min at room temperature with gentle rotation of the tubes. The coated beads were washed three times, with 200 μL of 20 mM PBS (pH 7.4) using magnetic separation. Finally, the immobilized CP (MB-CP) was resuspended in 20 mM PBS and kept at 4 °C until use.

2.4. Prehybridization and DNA strand displacement reaction

Prehybridized DNA strands were prepared by adding 5 μg mL^{-1} MB-CP with 10 μL of AuNP-RP and incubated for 20 min at 45 °C in a water-bath. Washing was performed 5 times with 20 mM PBS containing 0.05% Tween 20, and 3 times with 20 mM PBS.The supernatant was discarded, and the pellet of pre-hybridized DNA mix (containing AuNP-RP bound to MB-CP) was resuspended with 30 μL of target DNA in 20 mM PBS. This was used for DNA strand displacement. The reaction was incubated at 55 °C for 30 min. A magnet was used to separate the target DNA bound to MB-CP from the unbound (displaced) AuNP-RP and 5 μL of the supernatant was used for signal detection.

2.5. Detection of target DNA hybridization

DNA strand displacement and successful hybridization of the target DNA to MB-CP were detected using visual observation, spectrophotometry, and electrochemical methods. The supernatant containing unbound AuNP-RP was directly measured by each analytical method, without any washing step. The red color formation could be observed by the naked eye. For spectrophotometry detection, the absorbance of unbound AuNP in the supernatant was measured at 520 nm. The electrochemical measurement was

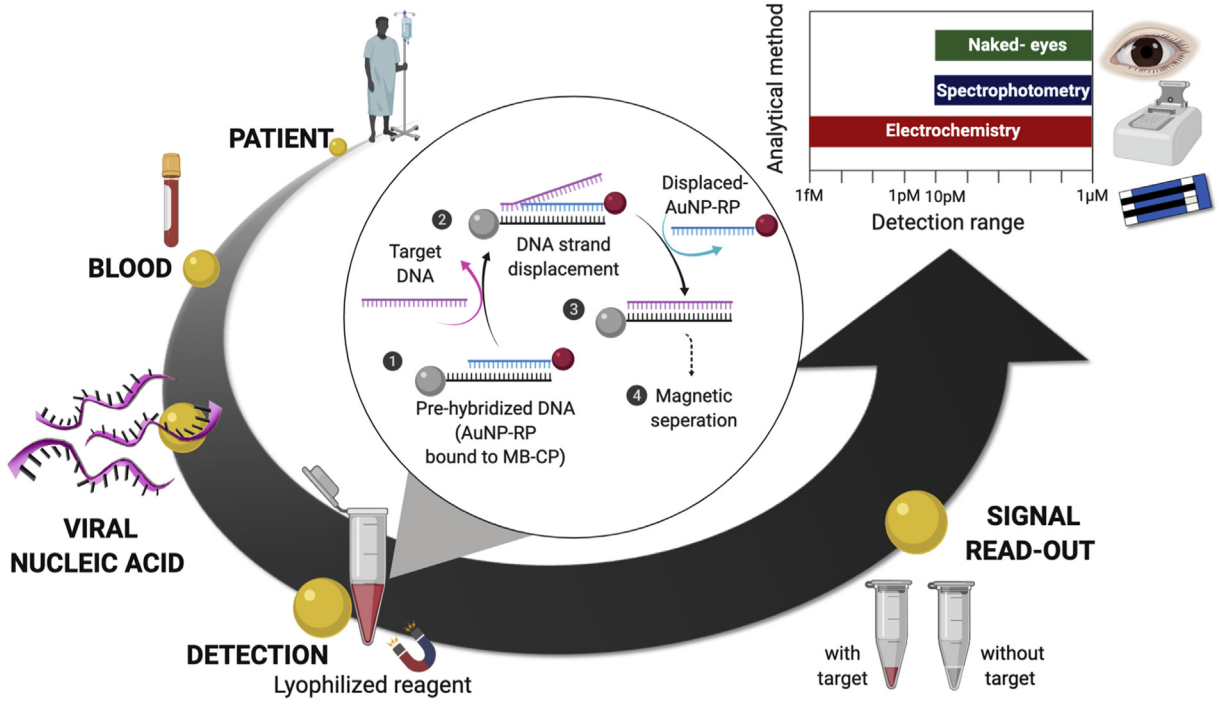

Scheme 1. Schematic illustration showing an overview of the one-pot detection of HEV using a DNA strand displacement reaction.

Table 1
Oligonucleotide sequences used in this study.

Oligonucleotide	Sequences (5′ to 3′)
Capture probe	5′-Biotin-GTC ACC CCA GAA ACC ACC GCC GG 3′
Reporter probe	5′-Thiol-GGT GGT TTC TGG GGT GAC 3′
Linear target DNA	5′ CCG GCG GTG GTT TCT GGG GTG AC 3′
1 base mismatched target DNA	5′ CCG GCA GTG GTT TCT GGG GTG AC 3′
3 bases mismatched target DNA	5′ CCG GCG GTG GTT TCT TTA GTG AC 3′
Biotin blocking probe	5′-Biotin- TTT TTT TTT T 3′
Thiol blocking probe	5′-Thiol- TTT TTT TTT T 3′
Non-complementary DNA (HAV)	5′ CGT TGA ATG GTT TTT GTC TTA ACA ACT CAC CAA TAT CCG CCG CTG TTA CC 3′
Non-complementary DNA (HBV)	5′ AAG ATG TTG TAC AGA CTT GGC CCC CAA TAC CAC ATC ATC CAT ATA ACT GAA AGC CAA 3′
Non-complementary DNA (HCV)	5′ CTG CGT GAA GAC AGT AGT TCC TCA CAG GGG AGT GAT TCA TGG TGG AGT GTC GCC C 3′

performed by pipetting 5 μL of the supernatant onto the working electrode surface of the SPCE followed by 50 μL of 1 M hydrobromic acid-bromine solution (HBr/Br_2). The AuNPs (Au^0) were oxidized to Au ions (Au^{3+}) by this strong acid. A differential pulse anodic stripping voltammetry (DPASV) technique was performed using a potentiostat (Metrohm-Autolab, Netherlands). The Au^{3+} ions were deposited on the surface of the working electrode by electrodeposition at −0.75 V for 100 s. This was followed by application of a step potential of 0.005 V with an interval time of 0.1 s, and modulation amplitude of 0.1 V for 0.05 s. For both spectrophotometry and electrochemical detection, the cut-off values were determined as + 3 standard deviations (3 SD) of the background signal.

2.6. Assay performance

The assay sensitivity was tested by varying the target DNA concentration from 0.1 fM to 1 μM. The assay specificity was evaluated with 100 pM of non-complementary DNA sequences, which were designed based on the genome sequences of hepatitis A (HAV), B (HBV), and C (HCV) viruses. Single-base and three-base mismatched sequences were also included.

2.7. Ready-to-use pre-hybridization mix in dry form

Pre-hybridized DNA strands were prepared as described in Section 2.4. After the washing step, the pellet was resuspended in 30 μL of 20 mM PBS containing 10% (w/v) sorbitol (pH 7.4) [26]. The pre-hybridization mix was lyophilized in a CentriVap Micro IR vacuum centrifugal concentrator (Labconco, USA) until completely dry. The tubes were sealed and kept in the dark with silica gel to prevent exposure to light and humidity. The lyophilized reagents' stability was evaluated under 3 different storage conditions (4 °C, 25 °C, and ambient temperature) for up to 3 months. At predetermined time points, the lyophilized reagent was reconstituted by adding 100 pM of target DNA solution in 30 μL of 20 mM PBS and measured using DPASV.

2.8. Detection of nucleic acid derived from HEV

To establish a simplified proof-of-concept in the ability for the DNA strand displacement assay to detect nucleic acid derived from a virus (HEV), viral RNA from an HEV-positive blood sample was extracted using the guanidinium thiocyanate-phenol-chloroform extraction method as previously described [27]. Complementary

DNA was synthesized using ImProm-II Reverse Transcription System (Promega, USA). Nested-PCR was performed to generate a PCR product (960 bp double-stranded DNA), which was purified using agarose gel electrophoresis. The concentration of the DNA was determined by measuring the absorbance at 260 nm using a Nanophotometer (NanoPhotometer N60, IMPLEN, USA). HEV-derived DNA (100 pM) and linear target DNA (100 pM) were used in the strand displacement reaction.

Human serum samples were spiked with the prepared DNA to simulate infected clinical sample. For controls, PBS buffer was used instead of a serum sample. Microwave irradiation [28] and microwave-Chelex methods were used for the extraction of DNA from the spiked serum samples. For both methods, the spiked serum was irradiated in a microwave oven (Samsung, Korea) at 800W for 5 min until it was desiccated. For the microwave irradiation method, sterile PBS was added to adjust the volume to 30 μL and used for the DNA strand displacement reaction. For the microwave-Chelex method, 5% (w/v) Chelex (Bio-Rad, USA) in PBS was added to a final volume of 30 μL and subsequently heated to 95 °C for 15 min. The resin was precipitated by centrifugation, and the clear supernatant was used for the DNA strand displacement reaction.

3. Results and discussion

3.1. The efficiency of AuNP conjugation to RP and MB immobilization of CP

The efficiency of AuNP conjugation to the DNA probes was determined by comparing the absorbance of DNA before and after conjugation. The amount of DNA attached to one AuNP was estimated to be ~16,000 molecules with a 60% loading efficiency (Table S1). The molar ratio of AuNPs and DNA was an important factor in determining the colloidal stability and DNA hybridization. A high surface density of DNA probes could potentially increase hybridization efficiency and facilitate the melting process, which are necessary for DNA hybridization [29]. On the other hand, high surface density may also cause steric hindrance [30], which was avoided by the use of thiol blocking probes containing poly T_{10} bases in this study.

The efficiency of CP immobilization on the surface of MB was measured using the absorbance at 260 nm. Approximately 73% of total DNA was immobilized on the MB, with a final concentration of 1.74 aM of MB-CP. The streptavidin MB was able to bind to biotinylated CP via a biotin-avidin interaction. An optimal ratio of DNA to MB is vital to avoid non-specific adsorption via electrostatic interactions of the exterior iron ions (especially Fe^{3+}) of MBs with the negative charge of the DNA phosphate backbone [18]. Therefore, biotinylated blocking probes containing poly T_{10} bases were used to minimize steric hindrance. The use of MB for the separation of bound and unbound DNA targets eliminated the need for multiple washing steps and resulted in a simplified procedure and reduced assay time [31,32].

3.2. Effect of MB-CP concentration on hybridization and DNA strand displacement reactions

The duration for magnetic separation of DNA bound to MB-CP from the unbound (displaced) AuNP-RP was optimized by varying the magnet application time from 30 to 180 s at each washing step. The result (Fig. S1) shows that there is no significant difference in the signal at 90 s and above ($p < 0.05$). Therefore, the shortest magnetic separation time was selected at 90 s to shorten the assay time and prevent non-specific binding/aggregation. Due to the large surface area of the magnetic beads, non-specific binding of AuNP-RP to its surface is possible. Fig. S2 shows the effect of sodium dodecyl sulphate (SDS) in the hybridization buffer on the current signal (A) and displacement efficiency (B). The current signal of the reaction without SDS was significantly higher ($p < 0.05$) than the reactions with SDS, possibly due to non-specific binding of AuNP-RP to the MB surface. The displacement efficiency of the reaction incorporated with SDS was significantly higher ($p < 0.05$) than the reaction without SDS. The addition of SDS in the hybridization buffer reduces non-specific hybridization and controls non-specific adsorption and variations in ionic strength via divalent Mg^{2+} or monovalent Na^{+} ions, which affect hybridization melting temperature and lead to enhancement of DNA hybridization kinetics and strand displacement [33,34]. Therefore, 0.1% (w/v) SDS was used as a surfactant in the hybridization buffer in all the experiments (Fig S2 B).

The concentrations of MB-CP were tested at 2.5, 5, 10, 15, and 20 μg mL^{-1} for pre-hybridization with 78 μg mL^{-1} of AuNP-RP, followed by target-induced strand displacement with 100 pM of the DNA target. The result showed an increase in the pre-hybridization electrochemical current signal when the concentration of MB-CP increased from 5 to 10 μg mL^{-1}, while there is no significant difference after 10 μg mL^{-1} ($p < 0.05$) (Fig. 1A). After target-induced strand displacement has occurred, the highest current signal was obtained with 5 mg mL^{-1} MB-CP, while the non-complementary target signal remained unchanged (Fig. 1B).

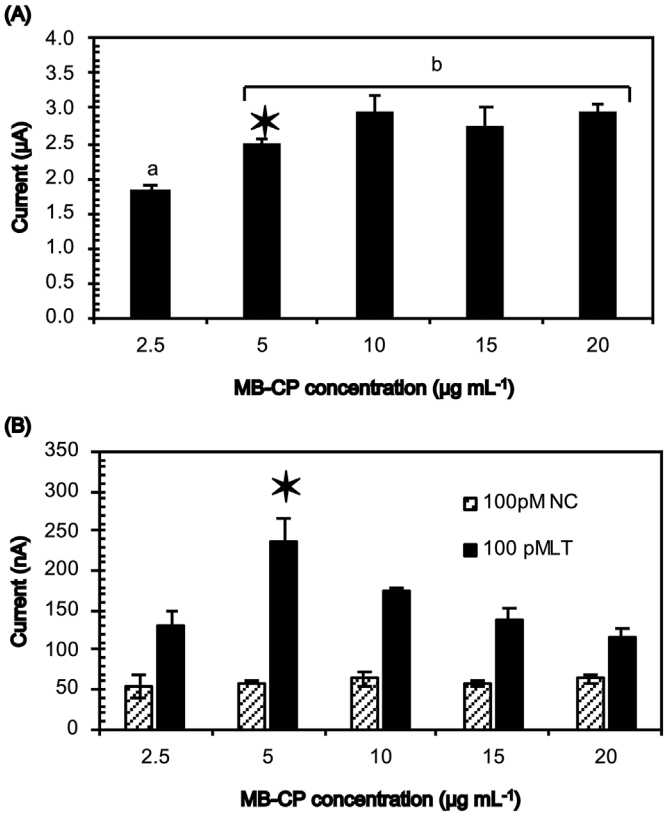

Fig. 1. Effect of different MB-CP concentrations on hybridization (A) and DNA strand displacement reactions (B). The prehybridization was performed using different concentrations of MB-CP and 78 μg mL^{-1} of AuNP-RP, while target-induced DNA strand displacement was performed with 100 pM of target DNA (LT) or non-complementary DNA (NC). The electrochemical current shown is the mean of 5 replicates ($n = 5$). Different letters indicate significant differences among different MB-CP concentrations (one-way ANOVA followed by Tukey HSD Test, $p < 0.05$). The star (*) above the bar chart represents the selected optimal point, which will be used for further experiments.

Concentration imbalances between duplex (pre-hybridized of MB-CP/AuRP) and target DNA have been used to drive the reactions by adjusting the new equilibrium concentrations of all constituents in the system [21]. Hence, concentration-disequilibrium force between the target DNA and duplex drives the adequate reaction of "Target DNA + MB-CP/AuRP → AuRP + MB-CP/target DNA" forward, leading to the enhancement of the displacement reaction. Thus, a more significant difference between the target and pre-hybridized DNA molar ratio resulted in faster kinetics.

3.3. Sensitivity and specificity of the assay

The sensitivity of the assay using visual observation, spectrophotometry, and electrochemical detection methods were determined. The red color of the AuNP-RP could clearly be detected by the naked eye from 10 pM to 1 μM of target DNA, while the absence of a red color (colorless read-out) was observed for 1 pM of target DNA, 100 pM NC and the blank (Fig. 2A). Spectrophotometry yielded a limit of detection (LOD) of 10 pM of target DNA, while the linear range was 1 pM to 1 μM ($R^2 = 0.94$) (Fig. 2C). Electrochemical detection gave a LOD of 1 fM of target DNA (3S/N), while the linear range was 1 pM to 1 μM ($R^2 = 0.97$) (Fig. 2D). The correlation between spectrophotometry and electrochemical detection yielded a R^2 value of 0.91, indicating a positive linear relationship between the 2 techniques over the range 1 pM to 1 μM (Fig. 2B). However, electrochemical detection was 10,000 times more sensitive than spectrophotometry. Thus, spectrophotometry and visual detection would be more suitable for the detection of samples with high target DNA concentration due to their simplicity and ease-of-use. These two detection methods are expected to facilitate the use of this assay in the field or laboratories with limited resources.

The sensitivity values obtained using the 3 detection methods were comparable to other studies that used a target-induced DNA displacement strategy and AuNPs as a signaling label (Table S2). Moreover, the use of magnetogenosensing in our assay greatly reduced the assay time to 30 min and increased sensitivity due to the higher surface area for probe immobilization. In addition, the assay did not require any multiple washing steps after target-induced DNA displacement and DNA immobilization on the electrode surface. The assay's specificity was evaluated using target and non-complementary DNA targets (HAV, HBV, and HCV). Although these viruses are from different viral families, their infection can cause inflammation of the liver, which in some instances could lead to liver cirrhosis or hepatocellular carcinoma. Therefore, distinguishing the different types of viral hepatitis is important in determining disease severity and treatment options.

The positive cut-off value for electrochemical detection was determined as 150 nA. From the experimental results (Fig. 3), all non-complementary DNA targets (HAV, HBV, HCV) were negative, while combinations of HEV DNA and non-complementary DNA yielded positive results. The assay could discriminate between perfectly complementary and mismatched (1 and 3 bases) sequences ($p < 0.05$). The signal of the mismatched targets was similar to the signal of non-complementary DNA targets (HAV, HBV,

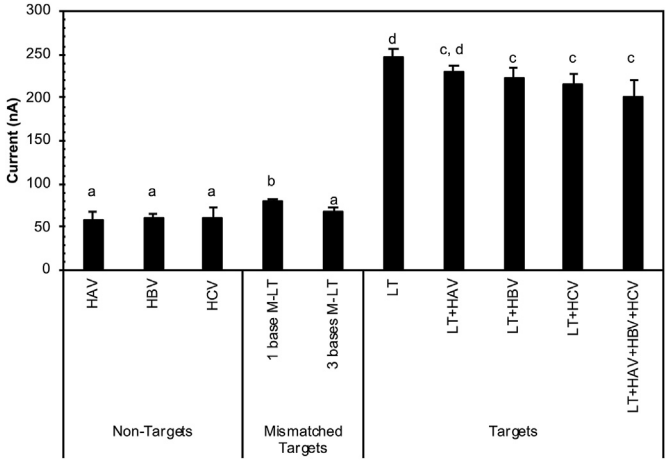

Fig. 3. The specificity of the assay based electrochemical detection. Complementary DNA linear target (LT), mismatched DNA linear targets (M-LT), and non-complementary targets (HAV, HBV, HCV) were used in this evaluation. The bar charts represent the mean of 5 replications DPASV measurement (n = 5). Lowercase letters denote homogenous subsets analyte by one-way ANOVA followed by Tukey HSD Test, $p < 0.05$.

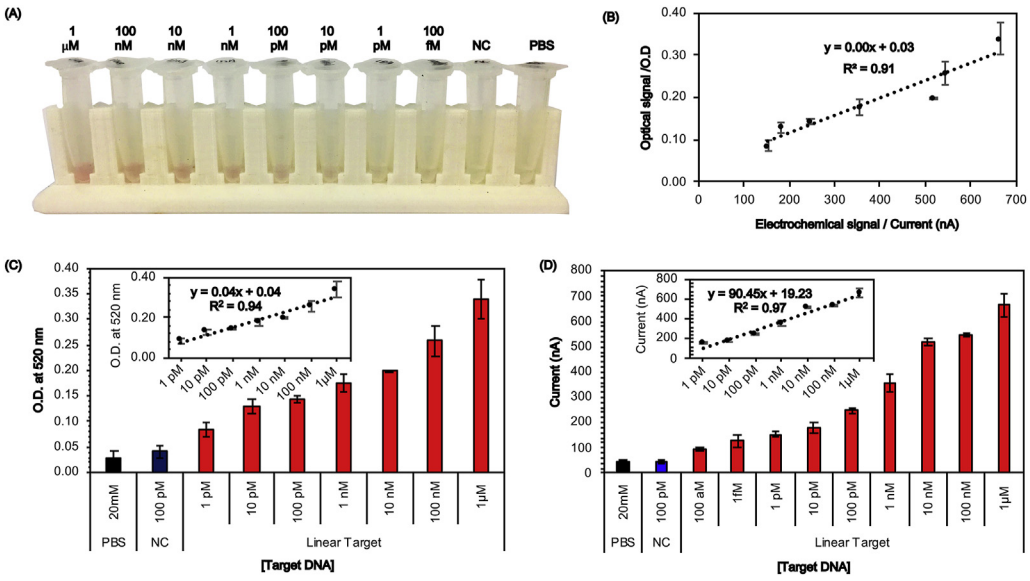

Fig. 2. The sensitivity of the assay based on the detection of the red color of AuNP-RP by visual observation (A), the correlation plot between spectrophotometry and electrochemical methods (B), by absorption spectrophotometry of AuNP at 520 nm (C) and by electrochemical detection (D). Collected data were from 5 replications (n = 5). (For interpretation of the references to color in this figure legend, the reader is referred to the Web version of this article.)

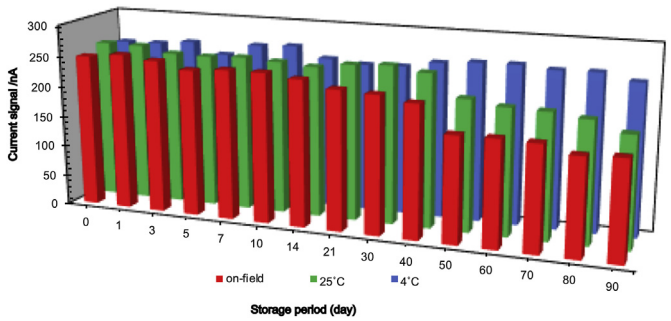

Fig. 4. The performance of the lyophilized pre-hybridization mix stored at 4 °C (blue), 25 °C (green), and outdoor ambient temperature (red) for three months. (For interpretation of the references to color in this figure legend, the reader is referred to the Web version of this article.)

HCV). In acute HEV infections, co-infection with multiple hepatitis viruses frequently occurs [5,35]. Therefore, this assay could be used to specifically detect HEV infection in the presence of a co-infection. On the other hand, a HEV-based serology test often suffers from cross-reactivity with other infectious agents, indicating a low positive predictive value of serological testing [36,37].

3.4. Stability of the lyophilized prehybridization mix

This work is the first report of a one-pot, ready-to-use lyophilized mix for HEV detection. The lyophilized mix is easy to store, transport and use in the field [17]. The dry form is ready-to-use and only requires the addition of the target DNA or sample to reconstitute it. This assay greatly reduces the assay complexity and the risk of cross-contamination from multiple pipetting steps.

In our study, sorbitol was used as the cryoprotectant based on a previous study, which selected sorbitol for lyophilization of DNA-conjugated gold nanoparticles [26]. Sugar is usually used as a cryoprotectant for the lyophilization of biomolecules and nanoparticles. Several hypotheses for the protective effects of sugars have been proposed, including a water replacement hypothesis, glass formation hypothesis, and kosmotropic effect.

A pre-hybridization mix, containing MB-CP hybridized to AuNP-RP and 10% sorbitol, was lyophilized to a dry form. The stability of the lyophilized form was evaluated at 4 °C, 25 °C, and outdoor ambient temperature to simulate the conditions in the field. The outdoor ambient temperature ranged from 24 to 34 °C, as recorded by the Thailand Meteorological Department (www.tmd.go.th) from August to November 2018.

The results from the stability study show that the pre-hybridization mix stored at 4 °C was stable for up to 3 months with no significant decrease in the current signal for 90 days. There were an 18% and 30% decrease in the current signal from the mix stored at 25 °C and outdoor ambient temperature for 50 days, respectively (Fig. 4). The drop in assay performance could be attributed to the denaturation of biomolecules due to increased temperature and humidity.

3.5. Detection of viral DNA

The 960 bp viral DNA could be detected using visual observation (Fig. 5A), spectrophotometry, and electrochemical detection (Fig. 5B). The correlation of the signal response from the longer strand RT-PCR amplicon with the short linear DNA target (23 bases) was ~93% and 100% for electrochemical and spectrophotometry measurements, respectively.

The World Health Organization (WHO) has established an international standard (IS) for HEV RNA (code number 6329/10), which is 5.39 $\log_{10}$ units mL^{-1} (95% CI 5.15–5.63), or 250,000 IU mL^{-1} [38]. In this study, the possible limit of detection using electrochemical and spectrophotometry (optical) detection is 4.26 $\log_{10}$ units mL^{-1} and 8.26 $\log_{10}$ units mL^{-1}, respectively. This result shows that our sensing platform could in principle detect the IS for HEV RNA detection.

The viral DNAand short linear DNA targets were then spiked into human serum samples or PBS buffer as a control, to mimic the procedure for nucleic acid detection in serum samples. Microwave-irradiation and microwave-Chelex methods were used in the nucleic acid extraction process from human serum. The DNA loss during the extraction process was determined using a UV–vis spectrophotometer at 260 nm, which were 14.54% and 7.41% for microwave-irradiation and microwave-Chelex method, respectively (data not shown). There may be some loss of DNA due to incomplete cell lysis, DNA degradation, or inefficient extraction procedures. The assay performances using spiked serum samples were expressed as the percentage of recovery, as shown in Table S3. The microwave-Chelex method resulted in higher recovery of long PCR amplicons than short linear DNA targets.

Further investigation revealed that the change in the reaction buffer's pH from neutral to basic during the extraction process using Chelex resin could lead to a higher displacement of the target

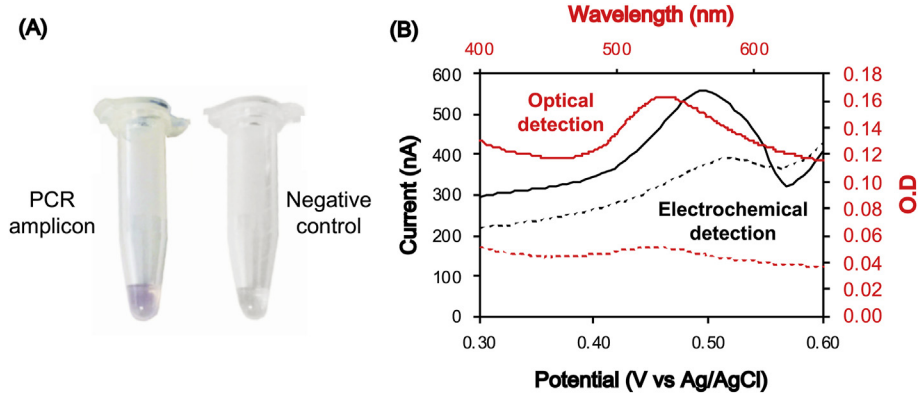

Fig. 5. Detection of HEV from patient serum sample using visual detection, spectrophotometry, and electrochemical detection. (A) Visual detection of a positive reaction containing displaced-AuRPs with 100 pM of RT-PCR amplicon (red color solution in a left tube) compared to the negative control (colorless solution in the right tube). (B) The measurement of displaced-AuRPs with 100 pM target amplicon (solid line) and non-complementary PCR product (dash line), voltammogram from DPASV technique is shown in black and absorbance spectra are shown in red. (For interpretation of the references to color in this figure legend, the reader is referred to the Web version of this article.)

DNA (Fig. S3). The percentage of displacement efficiency was reduced at lower pH compared to neutral or basic conditions. The change in pH can induce conformational changes in ssDNA, affecting its accessibility for hybridization [39]. At low pH (pH 4.0–6.0), ssDNA chains are stretched by a decrease of repulsive hydration forces between the phosphate groups on neighboring probe molecules due to H^+ protonation. In contrast, at high pH, the charged phosphate backbones of the ssDNA strands are fully deprotonated and electrostatic repulsion increases, leading to separation of the DNA strands and lower steric hindrance. Therefore, the target DNA has a higher chance of displacing the AuNP-RP from the MB-CP. This work demonstrates the potential application of this assay for real sample detection.

4. Conclusion

The development of a one-pot approach provides simplicity of detection using easily accessible techniques. Integrating the target DNA-induced displacement reaction, magnetic separation, and a thermo-stabilized reagent reduces the chances for carry-over contamination and pipetting error. The amount of displaced-AuNP-RP directly represents the amount of target DNA in the sample. Detection could be done by visual observation, spectrophotometry, and electrochemistry with good sensitivity and specificity. Furthermore, discrimination of either single base or three bases mismatched sequences could be achieved, which would be useful for mutation or genotyping studies. From a practical application point of view, the lyophilized dry reagent can be stored at 4 °C for up to 3 months without significant performance loss. Finally, this assay is easy to implement and could potentially be used for the detection of nucleic acid of viral or bacterial pathogens in infected samples.

CRediT authorship contribution statement

Tatchanun Ngamdee: Writing - original draft, Formal analysis, planned the experiments, planned the experiments, took the lead in writing and preparing the manuscript, All authors provided critical feedback and helped improve the research, analysis and manuscript. **Lee Su Yin:** Formal analysis, planned the experiments. **Sompong Vongpunsawad:** Formal analysis, contributed to sample preparation. **Yong Poovorawan:** Formal analysis, contributed to sample preparation. All authors contributed to the interpretation of the results. **Benchaporn Lertanantawong:** Writing - original draft, Formal analysis, conceived the idea, planned the experiments, planned the experiments, took the lead in writing and preparing the manuscript.

Declaration of competing interest

The authors declare that they have no known competing financial interests or personal relationships that could have appeared to influence the work reported in this paper.

Acknowledgements

The authors acknowledge the Center of Excellence in Clinical Virology, Faculty of Medicine, Chulalongkorn University, Bangkok, Thailand for providing the anonymous patient serum sample. T.N. acknowledges Petchra Pra Jom Klao Doctoral scholarship from KMUTT. B.L. greatly acknowledge the financial support Thailand Research Fund [Grant number: RSA6080050] and “KMUTT 55th Anniversary Commemorative Fund”.

Appendix A. Supplementary data

Supplementary data to this article can be found online at https://doi.org/10.1016/j.aca.2020.08.018.

Abbreviation

PCR	Polymerase chain reaction
NGS	next generation sequencing
ELISA	Enzyme-linked immunosorbent assay
LAMP	Loop-mediated isothermal amplification
SDS	sodium dodecyl sulphate
AuNPs	gold nanoparticles
HEV	hepatitis E virus
HAV	hepatitis A virus
HBV	hepatitis B virus
HCV	hepatitis C virus
MBs	magnetic bead nanoparticles
Fe_3O_4	(ferroferric oxide) nanoparticles
RP	reporter probes
CP	capture probes
SPCE	Screen-printed carbon electrode
PBS	phosphate buffer saline
DPASV	Differential pulse anodic stripping voltammetry
LT	linear target DNA
NC	non-complementary DNA
M-LT	mismatched DNA linear targets
HCR	hybridization chain reaction
TMSD	toehold-mediated DNA displacement reaction
SD-LAMP	strand displacement integrated loop mediated amplification
CSRP	circular strand-displacement polymerization
RSD	replication– scission–displacement

References

[1] R. Aggarwal, Diagnosis of hepatitis E, Nat. Rev. Gastroenterol. Hepatol. 10 (2013) 24–33, https://doi.org/10.1038/nrgastro.2012.187.
[2] N. Kamar, W. Wang, H.R. Dalton, Q. Pan, Direct-acting antiviral therapy for hepatitis E virus? Lancet Gastroenterol. Hepatol. 2 (2017) 154–155.
[3] P. Modesto, M.G. Maniaci, U. Cavallazzi, P.L. Acutis, S. Peletto, Evaluation of a molecular method for hepatitis E virus (HEV) detection in pancreatin of porcine origin, J. Virol Methods 276 (2020) 113790, https://doi.org/10.1016/j.jviromet.2019.113790.
[4] F. Marziali, J. Acosta, E. Bolatti, S. Mirazo, P. Skejich, P. Silva, J. Brassard, A. Costaguta, D. Gardiol, A.L. Cavatorta, Detection of HEV in naturally infected swine from central Argentina by an optimized HEV/MS2 duplex RT-qPCR, Zoonoses Public Health 66 (2019) 729–738, https://doi.org/10.1111/zph.12620.
[5] F. Qiu, J. Cao, Q. Su, Y. Yi, S. Bi, Multiplex hydrolysis probe real-time PCR for simultaneous detection of hepatitis A virus and hepatitis E virus, Int. J. Mol. Sci. 15 (2014) 9780–9788, https://doi.org/10.3390/ijms15069780.
[6] S.N. Chatterjee, P.B. Devhare, K.S. Lole, Detection of negative-sense RNA in packaged hepatitis E virions by use of an improved strand-specific reverse transcription-PCR method, J. Clin. Microbiol. 50 (2012) 1467, https://doi.org/10.1128/JCM.06717-11. LP – 1470.
[7] C. Choi, S.-K. Ha, C. Chae, Development of nested RT-PCR for the detection of swine hepatitis E virus in formalin-fixed, paraffin-embedded tissues and comparison with in situ hybridization, J. Virol Methods 115 (2004) 67–71, https://doi.org/10.1016/j.jviromet.2003.09.007.
[8] S. Gao, J. Wang, D. Li, Y. Li, C. Lou, E. Zha, X. Yue, Z. Tiezhong, Development and evaluation of a time-saving RT-qRPA method for the detection of genotype 4 HEV presence in raw pork liver, Int. J. Food Microbiol. 322 (2020) 108587, https://doi.org/10.1016/j.ijfoodmicro.2020.108587.
[9] F. Gerhardt, M. Maier, U.G. Liebert, U. Platzbecker, S.-Y. Wang, C.P. Papp, C.T. Bock, T. Berg, F. van Bömmel, Early detection of hepatitis E virus ribavirin resistance using next-generation sequencing, Antimicrob. Agents Chemother. 64 (2019), e01525-19, https://doi.org/10.1128/AAC.01525-19.
[10] L.P. Arce, M.F. Müller, A. Martinez, A. Baiker, G. Marranzino, F. Agote, M.G. Vizoso-Pinto, A novel in-house enzyme-linked immunosorbent assay for genotype 3 hepatitis E virus reveals high seroprevalence in blood donors in northern Argentina, Front. Microbiol. 10 (2019) 2481, https://doi.org/10.3389/fmicb.2019.02481.
[11] M.J. Ankcorn, S. Ijaz, B. Haywood, J. Neuberger, A.M. Elsharkawy, J. Maggs, R.S. Tedder, Confirmation of specificity of reactivity in a solid phase ELISA for

the detection of hepatitis E viral antigen improves utility of the assay, J. Virol Methods 252 (2018) 42–48, https://doi.org/10.1016/j.jviromet.2017.11.007.
[12] X. Lan, B. Yang, B.Y. Li, X.P. Yin, X.R. Li, J.X. Liu, Reverse transcription-loop-mediated isothermal amplification assay for rapid detection of hepatitis E virus, J. Clin. Microbiol. 47 (2009) 2304–2306, https://doi.org/10.1128/JCM.00498-09.
[13] Q. Chen, L. Yuan, J. Wan, Y. Chen, C. Du, Colorimetric detection of hepatitis E virus based on reverse transcription loop mediated isothermal amplification (RT-LAMP) assay, J. Virol Methods 197 (2014) 29–33, https://doi.org/10.1016/j.jviromet.2013.11.006.
[14] P. He, Y. Xu, Y. Fang, A review: electrochemical DNA biosensors for sequence recognition, Anal. Lett. 38 (2005) 2597–2623, https://doi.org/10.1080/00032710500369794.
[15] E. Boisselier, D. Astruc, Gold nanoparticles in nanomedicine: preparations, imaging, diagnostics, therapies and toxicity, Chem. Soc. Rev. 38 (2009) 1759–1782, https://doi.org/10.1039/B806051G.
[16] Y. Du, S. Dong, Nucleic acid biosensors: recent advances and perspectives, Anal. Chem. 89 (2017) 189–215, https://doi.org/10.1021/acs.analchem.6b04190.
[17] K.-F. Low, A. Karimah, C.Y. Yean, A thermostabilized magnetogenosensing assay for DNA sequence-specific detection and quantification of Vibrio cholerae, Biosens. Bioelectron. 47 (2013) 38–44, https://doi.org/10.1016/j.bios.2013.03.004.
[18] L. Ma, N. Sun, Y. Meng, C. Tu, X. Cao, Y. Wei, L. Chu, A. Diao, Harnessing the affinity of magnetic nanoparticles toward dye-labeled DNA and developing it as an universal aptasensor revealed by lipopolysaccharide detection, Anal. Chim. Acta 1036 (2018) 107–114, https://doi.org/10.1016/j.aca.2018.06.060.
[19] Z.Q. Chen, Y. Liu, C. Xin, J.K. Zhao, S.F. Liu, A cascade autocatalytic strand displacement amplification and hybridization chain reaction event for label-free and ultrasensitive electrochemical nucleic acid biosensing, Biosens. Bioelectron. 113 (2018) 1–8, https://doi.org/10.1016/j.bios.2018.04.046.
[20] J.Y. Song, P. Su, R.A. Ma, Y. Yang, Based on DNA strand displacement and functionalized magnetic nanoparticles: a promising strategy for enzyme immobilization, Ind. Eng. Chem. Res. 56 (2017) 5127–5137, https://doi.org/10.1021/acs.iecr.7b00595.
[21] D. Yao, T. Song, X. Sun, S. Xiao, F. Huang, H. Liang, Integrating DNA-strand-displacement circuitry with self-assembly of spherical nucleic acids, J. Am. Chem. Soc. 137 (2015) 14107–14113, https://doi.org/10.1021/jacs.5b07453.
[22] Y.Q. He, K. Zeng, X.B. Zhang, A.S. Gurung, M. Baloda, H. Xu, G.D. Liu, Ultrasensitive electrochemical detection of nucleic acid based on the isothermal strand-displacement polymerase reaction and enzyme dual amplification, Electrochem. Commun. 12 (2010) 985–988, https://doi.org/10.1016/j.elecom.2010.05.007.
[23] F. Wang, C.H. Lu, I. Willner, From cascaded catalytic nucleic acids to enzyme-DNA nanostructures: controlling reactivity, sensing, logic operations, and assembly of complex structures, Chem. Rev. 114 (2014) 2881–2941, https://doi.org/10.1021/cr400354z.
[24] J.J. Jiang, X.Y. Lin, D. Ding, G.W. Diao, Enzyme-free homogeneous electrochemical biosensor for DNA assay using toehold-triggered strand displacement reaction coupled with host-guest recognition of Fe3O4@SiO2@beta-CD nanocomposites, Biosens. Bioelectron. 114 (2018) 37–43, https://doi.org/10.1016/j.bios.2018.04.035.
[25] J. Liu, Y. Lu, Preparation of aptamer-linked gold nanoparticle purple aggregates for colorimetric sensing of analytes, Nat. Protoc. 1 (2006) 246, https://doi.org/10.1038/nprot.2006.38.
[26] P.S. Liew, B. Lertanantawong, S.Y. Lee, R. Manickam, Y.H. Lee, W. Surareungchai, Electrochemical genosensor assay using lyophilized gold nanoparticles/latex microsphere label for detection of Vibrio cholerae, Talanta 139 (2015) 167–173, https://doi.org/10.1016/j.talanta.2015.02.054.
[27] D. Intharasongkroh, T. Thongmee, P. Sa-nguanmoo, S. Klinfueng, A. Duang-in, R. Wasitthankasem, A. Theamboonlers, U. Charoonruangrit, S. Oota, S. Payungporn, S. Vongpunsawad, C. Chirathaworn, Y. Poovorawan, Hepatitis E Virus Infection in Thai Blood Donors, 2018, https://doi.org/10.1111/trf.15041, 0.
[28] A.W. Tam, M.M. Smith, M.E. Guerra, C.-C. Huang, D.W. Bradley, K.E. Fry, G.R. Reyes, Hepatitis E virus (HEV): molecular cloning and sequencing of the full-length viral genome, Virology 185 (1991) 120–131, https://doi.org/10.1016/0042-6822(91)90760-9.
[29] H. Pei, F. Li, Y. Wan, M. Wei, H.J. Liu, Y. Su, N. Chen, Q. Huang, C.H. Fan, Designed diblock oligonucleotide for the synthesis of spatially isolated and highly hybridizable functionalization of DNA-gold nanoparticle nanoconjugates, J. Am. Chem. Soc. 134 (2012) 11876–11879, https://doi.org/10.1021/ja304118z.
[30] S.J. Hurst, A.K.R. Lytton-Jean, C.A. Mirkin, Maximizing DNA loading on a range of gold nanoparticle sizes, Anal. Chem. 78 (2006) 8313–8318, https://doi.org/10.1021/ac0613582.
[31] H.Y. Lau, H. Wu, E.J.H. Wee, M. Trau, Y. Wang, J.R. Botella, Specific and sensitive isothermal electrochemical biosensor for plant pathogen DNA detection with colloidal gold nanoparticles as probes, Sci. Rep. 7 (2017).
[32] X.-M. Li, L.-L. Wang, J. Luo, Q.-L. Wei, A dual-amplified electrochemical detection of mRNA based on duplex-specific nuclease and bio-bar-code conjugates, Biosens. Bioelectron. 65 (2015) 245–250.
[33] K. Rose, J.O. Mason, R. Lathe, Hybridization parameters revisited: solutions containing SDS, Biotechniques 33 (2002) 54–58, https://doi.org/10.2144/02331st01.
[34] R.F. Nitu, S.J. Burns, M. Ionită, Oligonucleotide detection and optical measurement with graphene oxide in the presence of bovine serum albumin enabled by use of surfactants and salts, Coatings 10 (2020), https://doi.org/10.3390/coatings10040420.
[35] K.-T. Wu, K.-M. Chung, I.-C. Feng, M.-J. Sheu, H.-T. Kuo, L.-B. Koay, C.-Y. Lin, L.-Y. Tang, S.-L. Tsai, Acute hepatitis E virus infection in Taiwan 2002–2006 revisited: PCR shows frequent co-infection with multiple hepatitis viruses, J. Med. Virol. 81 (2009) 1734–1742, https://doi.org/10.1002/jmv.21442.
[36] N.W. Furukawa, E.H. Teshale, L. Cosmas, M. Ochieng, S. Gikunju, B.S. Fields, J.M. Montgomery, Serologic evidence for hepatitis E virus infection among patients with undifferentiated acute febrile illness in Kibera, Kenya, J. Clin. Virol. 77 (2016) 106–108, https://doi.org/10.1016/j.jcv.2016.02.021.
[37] K. Parvez, R. Ali, Hepatitis E virus cross-reactivity and false-seropositivity: challenges to diagnosis, J. Liver 3 (2014), https://doi.org/10.4172/2167-0889.1000e109.
[38] S.A. Baylis, J. Blumel, S. Mizusawa, K. Matsubayashi, H. Sakata, Y. Okada, C.M. Nubling, K.M.O. Hanschmann, H.E.V.C.S. Grp, World Health organization international standard to harmonize assays for detection of hepatitis E virus RNA, Emerg. Infect. Dis. 19 (2013) 729–735, https://doi.org/10.3201/eid1905.121845.
[39] J. Zhang, H.P. Lang, G. Yoshikawa, C. Gerber, Optimization of DNA hybridization efficiency by pH-driven nanomechanical bending, Langmuir 28 (2012) 6494–6501, https://doi.org/10.1021/la205066h.